Available online at www.sciencedirect.com
SCIENCE DIRECT®
Bioorganic & Medicinal Chemistry Letters 16 (2006) 507–511
Bioorganic & Medicinal Chemistry Letters

Guiding farnesyltransferase inhibitors from an ECLiPS® library to the catalytic zinc

Chia-Yu Huang,[a] Tara M. Stauffer,[a] Corey L. Strickland,[b] John C. Reader,[a] He Huang,[a] Ge Li,[a] Alan B. Cooper,[b] Ronald J. Doll,[b] Ashit K. Ganguly,[b] John J. Baldwin[a] and Laura L. Rokosz[a,*]

[a]*Pharmacopeia Drug Discovery, PO Box 5350, Princeton, NJ 08543-5350, USA*
[b]*Schering-Plough Research Institute, 2015 Galloping Hill Rd., Kenilworth, NJ 07033-1300, USA*

Received 9 September 2005; revised 18 October 2005; accepted 19 October 2005
Available online 10 November 2005

Abstract—Farnesyltransferase inhibitors identified from an ECLiPS® library were optimized using solution-phase synthesis. X-ray crystallography of inhibited complexes was used to identify substructures that coordinate to the active site zinc. The X-ray structures were ultimately used to guide the design of second-generation analogs with FTase IC_{50}s of less than 1.0 nM.

Farnesyltransferase (FTase) is a compelling therapeutic target in the field of oncology as it is specifically linked to the aberrant behavior of tumor cells.[1] The tricyclic drug, **SCH 66336** (Sarasar, Fig. 1), was the first FTase inhibitor (FTI) to enter the clinic, resulting in favorable outcomes in a number of solid tumor types and hematological malignancies.[2] The significant synergy with taxanes in inhibiting tumor growth makes this chemical class of FTIs particularly intriguing.[3]

A collection of FTIs that are structurally related to **SCH 66336**, identified from FT-1, a 11,718-member ECLiPS® (Encoded Combinatorial Library on Polymeric Support) library, has been described recently.[4] The most potent hits from FT-1 contained a 3-bromo-8-chlorobenzocyclohepta-pyridine ring attached to a piperazine core with 3-pyridylmethylamide or alkyl amides at position 2 and phenylpropanamide or 4-pyridylacetamide at position 1. Examples of such compounds are represented by **1** and **2** (Fig. 2, Scheme 1). The substituents at position 2 make these compounds unique since this is a site that had never previously been explored. To further define the SAR at these positions, several smaller collections of analogs were made. These synthetic efforts also constituted an attempt to identify substituents that could make a comparable contribution to the potency as that afforded by the bromine at position C-10 of tricyclic FTIs such as **SCH 66336** (Fig. 1).[5,6]

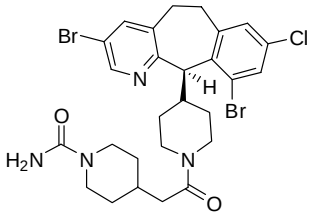

Figure 1. SCH 66336, Sarasar, FTase IC_{50} = 1–2 nM.[2b]

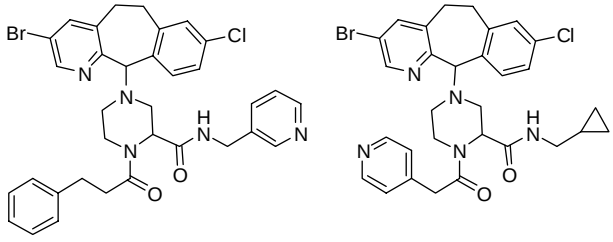

Figure 2. Resynthesized compounds from the ECLiPS library, FT-1.

Keywords: Anti-cancer; Catalytic zinc; Farnesyltransferase; Rational drug design; Solution-phase synthesis; X-ray crystallography.
* Corresponding author. Tel.: +1 609 452 3718; fax: +1 609 655 4187; e-mail: rock@pcop.com

0960-894X/$ - see front matter © 2005 Elsevier Ltd. All rights reserved.
doi:10.1016/j.bmcl.2005.10.070

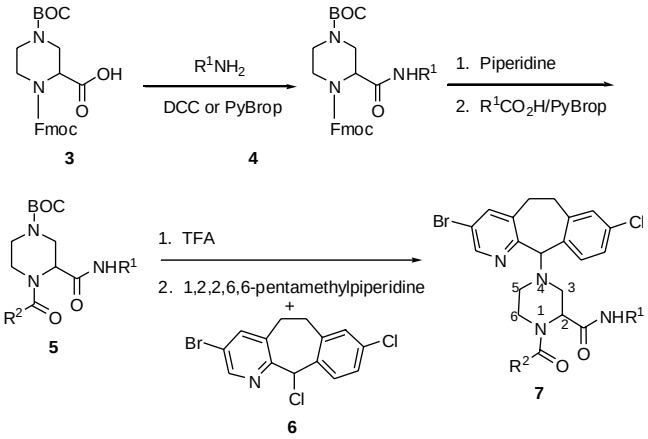

Scheme 1. General synthetic procedure for synthesis of the FT-1 analogs.

The first collection, synthesized as shown in Scheme 1, contained 3-pyridylmethylamide at the 2-position of the piperazine core since this was a frequently seen feature of the most potent compounds retrieved from the FT-1 screen.[4] Starting from *N*-1-Fmoc *N*-4-Boc piperazine-2-carboxylic acid **3**, coupling of 3-pyridylmethylamine using DCC or PyBrop gave amide **4**. Removal of the Fmoc group and coupling with various acids using PyBrop resulted in compound **5**. After deprotection of the Boc group with TFA, the neutralized amine was reacted with previously reported[7] chloride **6** to afford compound **7**. The compounds were tested in the same scintillation proximity assay (SPA) used to screen FT-1.[4] Since the FTase concentration is 2.8 nM, the lower limit of sensitivity for IC_{50} determinations is approximately 5 nM. To further supplement our ability to rank-order the compounds, all compounds were also evaluated in a COS cell Ha-Ras processing assay.[8]

Both acyclic (**8**–**11**) and cyclic amides (**12**–**14**) are well tolerated (Table 1) with IC_{50}s of less than 20 nM. The cyclic amides show a smaller separation between enzyme and cell activity suggesting better whole-cell penetration.

Elaboration of the acyclic amides at R^2 revealed a tolerance for many functional groups on the distal end of this position, such as carboxylic acid (**15**), ketones (**16**–**18**), ethers (**19**, **20**), ester (**21**), amide (**22**), and carbamate (**23**). The tertiary amide, **22**, is remarkable in that the enzyme IC_{50} (13 ± 1.4 nM) and the COS IC_{50} (11 ± 1.5) are nearly identical. This suggests that the amide chemotype has a lower threshold for cell penetration. The carboxylic acid, **15**, and the carbamate, **23**, show a much higher threshold for cell penetration. Nonetheless, the potency of **23** in the enzyme assay ($IC_{50} = 22 \pm 3.5$) prompted us to explore other related functionalities, such as urea.

Acyclic (**24**–**28**) and cyclic (**29**–**33**) ureas were prepared using a procedure similar to Scheme 1, except that isocyanates were used in place of carboxylic acids at R^2. The most potent compound is the cyclohexylurea **30**, with an enzyme IC_{50} of 5.5 ± 0.7 nM and a COS IC_{50} of 8.6 ± 0.2 nM. Not only is **30** the most potent of the ureas but it also shows the smallest separation between the enzyme and COS assay IC_{50}s.

Table 1. Elaboration of the N-1 position of core **7** (R^1 = 3-pyridylmethyl)

Compound	R^2	FTase IC_{50} (nM) ±SD	COS IC_{50} (nM) ±SD
8	$Me(CH_2)_2CH_2$–	5.7 ± 2.1	64 ± 6
9	$Me(CH_2)_3CH_2$–	8.0 ± 1.2	75 ± 2
10	Me_2CHCH_2–	7.3 ± 0.7	50 ± 0
11	Me_3CCH_2–	12 ± 0.4	120 ± 23
12	Cycloheptyl–	12 ± 3.0	85 ± 9
13	Cyclohexylethyl–	20 ± 7	38 ± 12
14	Cyclopentyl–	17 ± 6.0	65 ± 21
15	$HO_2C(CH_2)_2CH_2$–	7.0 ± 0.6	>200
16	$MeC(O)(CH_2)_3CH_2$–	8.0 ± 0.3	49 ± 15
17	$MeC(O)(CH_2)_2CH_2$–	8.4 ± 0.9	54 ± 2
18	$MeC(O)CH_2CH_2$–	11 ± 3.0	47 ± 2
19	$MeOCH_2CH_2$–	20 ± 5.3	100 ± 0
20	$MeCH_2OCH_2$–	21 ± 8.5	160 ± 12
21	$MeOC(O)(CH_2)_3CH_2$–	7.9 ± 0.4	62 ± 2
22	$Me_2NC(O)CH_2CH_2$–	13 ± 1.4	11 ± 2
23	Me_3CO–	22 ± 3.5	>200
24	$CH_3(CH_2)_3NH$–	9.1 ± 1.4	45
25	$CH_3(CH_2)_2NH$–	19 ± 1	59 ± 17
26	Me_2CHCH_2NH–	8.0 ± 1.3	52 ± 37
27	Me_2CHNH–	47 ± 5	140 ± 1
28	Me_3CNH–	15 ± 2	54 ± 4
29	Cycloheptyl-NH–	9.1 ± 0.5	52 ± 26
30	Cyclohexyl-NH–	5.5 ± 0.7	8.6 ± 0.2
31	Cyclohexylmethyl-NH–	10 ± 1.3	53 ± 8
32	Cyclopentyl-NH–	14 ± 8	28 ± 1.5
33	Cyclopropyl-NH–	51 ± 4.2	260 ± 46

A trihalogenated analog of compound **8**, containing an additional bromine at position 10 of the tricycle, demonstrates comparable enzyme activity (FTase $IC_{50} = 5.6 \pm 2.4$ nM) but improved COS activity (COS $IC_{50} = 5.3 \pm 0.0$ nM). X-ray crystallography of FTase inhibited with this compound showed that the 3-pyridylmethyl side chain interacts with the active site zinc (Fig. 3). The distance between the pyridine nitrogen and the zinc atom is 2.29 Å. This finding makes this series of compounds particularly noteworthy since the tricyclic FTI, **SCH 66336**, does not contain substituents that are capable of zinc coordination.[10] The X-ray structure thus suggested that other zinc ligands would be suitable replacements for this substituent. Fixing R^2 as butyl, a survey of R^1 modifications such as pyridines (**34**, **35**), pyrazine (**36**), isoxazole (**37**), and ethyl- or methyl-imidazoyl (**38**–**40**) indicated that while all but the pyridine N-oxide, **34**, were tolerated, the imidazoylethyl, as exemplified by **38**, was most preferred yielding an enzyme IC_{50} of 12 ± 3.6 nM and a COS IC_{50} of 60 ± 15 nM (Table 2).

Given the potent enzyme and cell-based activity of the cyclohexylurea, **30** (Table 1), we sought to combine this pharmacophore with those of the imidazoyls in Table 2. As shown in Table 3, imidazoylpropyl (**41**, **42**) or imidazoylethyl (**43**, **44**) containing compounds, along with the 2-oxo-pyrrolidinylpropyl compound, **46**, are comparable in both enzyme and COS activity to that of the 3-pyridylmethyl compound, **30**. Compound **41**

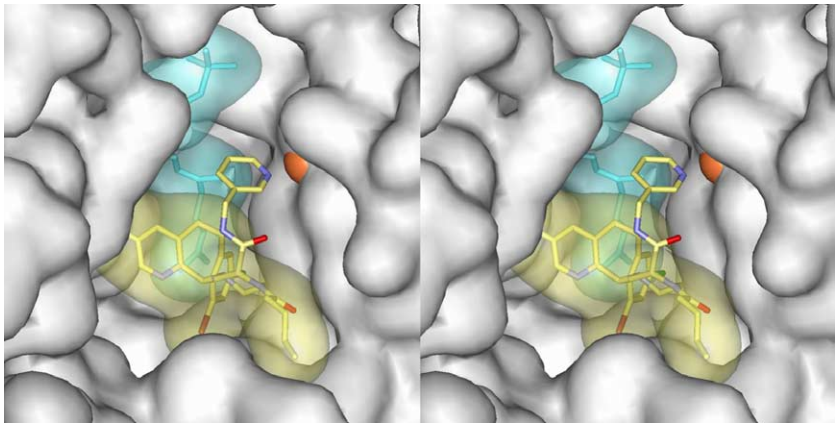

Figure 3. X-Ray structure of the FTase complex with a 10-Br analog (FTase IC_{50} = 5.6 ± 2.4 nM, COS IC_{50} = 5.3 ± 0.0 nM) of **8**.[9] The zinc atom at the active site is represented by the red ball.

Table 2. Pyridine replacements at the C-2 position of core **7** (R^2 = butyl)

Compound	R^1	FTase IC_{50} (nM) ±SD	COS IC_{50} (nM) ±SD
8	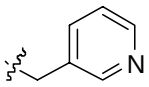	5.7 ± 2.1	64 ± 6
34	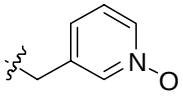	1800 ± 570	>200
35	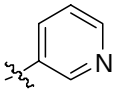	18 ± 2	100 ± 30
36	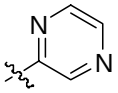	190 ± 14	570 ± 180
37	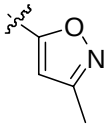	560 ± 20	>4500
38	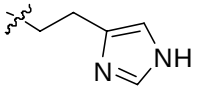	12 ± 4	60 ± 15
39	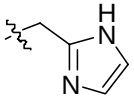	80 ± 4	>200
40	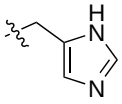	45 ± 19	210 ± 7

(a mixture of four isomers) is the most potent in this collection with IC_{50}s in both the enzyme and COS assay of less than 5.0 nM. The potency in the enzyme assay is predicted to be greater as it appears to be beyond the limit of sensitivity for the FTase SPA assay.

Since it is known that the (*R*) isomer is the preferred configuration at the C-2 position of the piperazine

Table 3. Analogs of **38** (Core **7** where R^2 = cyclohexyl-NH–)

Compound	R^1	FTase IC_{50} (nM) ±SD	COS IC_{50} (nM) ±SD
41	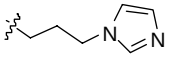	4.5 ± 2.3	4.2 ± 0.2
42	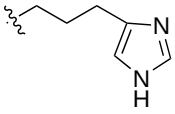	13 ± 1.7	9.7 ± 1.4
43	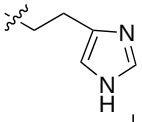	7.0 ± 0.4	18 ± 8.7
44	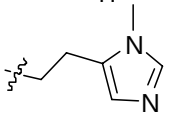	7.3 ± 2.9	13 ± 17
45	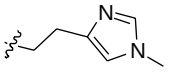	26 ± 7.7	91 ± 17
46	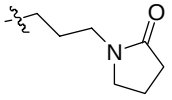	14 ± 1.5	20 ± 0.3
47	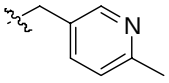	61 ± 20	550
48	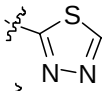	490 ± 130	>10,000
49	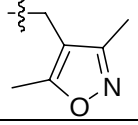	760 ± 250	Not tested

core[11], compound **41** was prepared using (*R*)-piperazine-2-carboxylic acid to give a diastereomeric mixture and subsequently separated by HPLC to give **41a** and **41b** (Table 4). The absolute configuration at C-11 of the tricyclic piece was not determined but the findings of Strickland et al.[5] suggest that the stereochemistry at this position does not have a significant impact on

Table 4. Biological evaluation of the purified isomers of **41**

Compound[a]	FTase IC_{50} (nM)[b]	GGTase I IC_{50} (nM)[c]	COS IC_{50} (nM) ±SD	Soft Agar IC_{50} (nM) ±SD	Rat liver microsome stability[d]
41a	V_1 = 2.0 V_2 = 0.10 ± 0.04	22,000	1.2 ± 0.3	5.2 ± 1.0	>95%
41b	V_1 = 1.5	>10,000	0.56 ± 0.06	5.0 ± 0.6	>95%

[a] Compound **41** was prepared as a diastereomeric mixture and was subsequently resolved by HPLC. Compound **41a** is the first-eluting isomer and **41b** is the second-eluting isomer.
[b] The V_1 FTase IC_{50} was quantified as described in Rokosz et al.[4] The V_2 FTase IC_{50} was quantified as described in Ref. 12.
[c] GGTase I activity was measured as described by Bishop et al.[8] All other assays were conducted as described in the References and notes section.
[d] The microsome stability is defined as the percent of compound remaining following treatment with microsomes as described.[14]

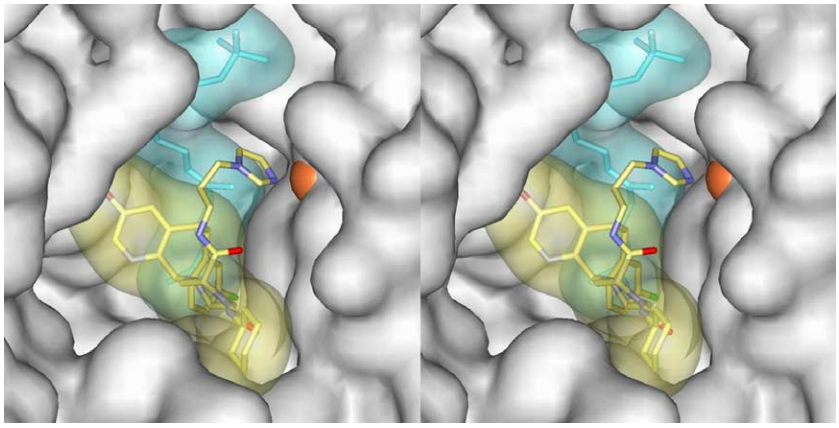

Figure 4. X-ray crystal structure of 41b bound to FTase. The zinc atom at the active site is represented by the red ball.

enzyme activity. The less polar isomer, **41a**, was arbitrarily designated as isomer 1, while the more polar isomer, **41b**, was designated as isomer 2. As expected, the purified isomers show identical activities in both the enzyme and COS assays (IC_{50}s $\leqslant$ 2.0 nM). To obtain a more accurate enzyme IC_{50} compound **41a** was re-tested in a modified version of the SPA assay, with improved sensitivity (V_2).[12] This assay yielded an IC_{50} for **41a** of 0.10 ± 0.04 nM. This potency is consistent with that reported by Taveras et al.[10] A soft agar assay was used to determine if the compounds can reverse the adherent-independent phenotype of the transformed cell line, NIH-3T3.[13] Both isomers produced soft agar IC_{50}s of 5.0 nM. They are also greater than 10,000-fold selective for FTase over geranylgeranyltransferase I (GGTase I). In order to assess metabolic stability, the isomers were incubated with rat liver microsomes for 1 h at 37 °C.[14] Both compounds remained largely (>95%) intact under these conditions. A mouse pharmacokinetic study was used to show that **41b** has an AUC (area under the curve) of 1.66 μg/ml h and a C_{max} of 2.55 μM (10 mpk in 20% HPβCD, po). However, the overall bioavailability, when compared to the plasma levels of intravenous dosing, was just 10.6%. Metabolism is likely due to peptidic cleavage at the amide bond. This reaction can be tempered via conversion of the secondary nitrogen at the amide bond to a tertiary nitrogen.[10,15]

X-ray crystal analysis of FTase inhibited with **41b** (Fig. 4) shows that the imidazole moiety interacts, as expected, with the catalytic zinc in the active site. The distance between the imidazole and the zinc atom is 2.08 Å. Taken together, these data suggest that the enhancement in potency afforded through interaction with the active site zinc is comparable to, if not greater than, that contributed through the addition of a bromine at the C-10 position of the tricycle. Further structural details of the FTase-**41b** complex will be reported in due course.

Acknowledgments

We are grateful to Jagdish Desai for the synthesis of the tri-halogenated compound shown in Figure 3 and to Amin Nomeir for pharmacokinetic evaluation of **41b**. We would like to express our sincere appreciation to Dr. Matthew Sills for critical review of the manuscript.

References and notes

1. (a) Doll, R. J.; Kirschmeier, P.; Bishop, W. R. *Curr. Opin. Drug Discovery Dev.* **2004**, *7*, 478; (b) Dancey, J. E. *Curr. Pharm. Des.* **2002**, *8*, 2259; (c) Kohl, N. E. *Ann. N. Y. Acad. Sci.* **1999**, *886*, 91; (d) Gibbs, J. B.; Oliff, A. *Ann. Rev. Pharmacol. Toxicol.* **1997**, *37*, 143.
2. (a) O'Regan, R. M.; Khuri, F. R. *Endocr. Relat. Cancer* **2004**, *11*, 191; (b) Bishop, W. B.; Kirschmeier, P.; Baum, C. *Cancer Biol. Ther.* **2003**, *9*, 73; (c) Caponigro, F.; Casale, M.; Bryce, J. *Exp. Opin. Invest. Drugs* **2003**, *12*, 946; (d) Head, J. E.; Johnston, S. R. D. *Exp. Opin. Emerg. Drugs* **2003**, *8*, 168; (e) Kelland, L. R. *Exp. Opin. Invest. Drugs* **2003**, *12*, 417; (f) Haluska, G. K.; Dy, G. K.; Adjei, A. A. *Eur. J. Cancer* **2002**, *38*, 1685.
3. (a) Nielsen, L. L.; Shi, B.; Hajian, G.; Yaremko, B.; Lipari, P.; Farrari, E.; Gurnani, M.; Malkowski, M.; Chen, J.;

Bishop, W. R.; Liu, M. *Cancer Res.* **1999**, *59*, 5896; (b) Wang, E.; Casiano, C. N.; Clement, R. P.; Johnson, W. W. *Cancer Res.* **2001**, *61*, 7525; (c) Hoover, R. R.; Mahon, F.; Melo, J. V.; Daley, G. Q. *Blood* **2002**, *100*, 1068; (d) Caponigro, F. *Anti-Cancer Drugs* **2002**, *13*, 891.

4. Rokosz, L. L.; Huang, C-Y.; Stauffer, T. M.; Reader, J. C.; Chelsky, D.; Sigal, N. H..; Ganguly, A. K.; Baldwin, J. J. *Bioorg. Med. Chem. Lett*. **2005,** *15*, 5537.
5. Strickland, C. L.; Weber, P. C.; Windsor, W. T.; Wu, Z.; Le, H. V.; Albanese, M. M.; Alvarez, C. S.; Cesarz, D.; del Rosario, J.; Deskus, J.; Mallams, A. K.; Njoroge, F. G.; Piwinski, J. J.; Remiszewski, S.; Rossman, R. R.; Taveras, A. G.; Vibulbhan, B.; Doll, R. J.; Girijavallabhan, V. M.; Ganguly, A. K. *J. Med. Chem.* **1999**, *42*, 2125.
6. Njoroge, F. G.; Taveras, A. G.; Kelly, J.; Remiszewski, S.; Mallams, A. K.; Wolin, R.; Afonso, A.; Cooper, A. B.; Rane, D. F.; Liu, Y. T.; Wong, J.; Vibulbhan, B.; Pinto, P.; Deskus, J.; Alvarez, C. S.; del Rosario, J.; Connolly, M.; Wang, J.; Desai, J.; Rossman, R. R.; Bishop, W. R.; Patton, R.; Wang, L.; Kirschmeier, P.; Ganguly, A. K. *J. Med. Chem.* **1998**, *41*, 4890.
7. Njoroge, F. G.; Vibulbhan, B.; Pinto, P.; Strickland, C.; Kirschmeier, P.; Bishop, W. R.; Girijavallabhan, V. *Bioorg. Med. Chem. Lett.* **2004**, *14*, 5877, and references therein.
8. Ha-Ras processing in COS-7 African, green monkey kidney cells was conducted as described in Bishop, W. B.; Bond, R.; Petrin, J.; Wang, L.; Patton, R.; Doll, R.; Njoroge, G.; Catino, J.; Schwartz, J.; Windsor, W.; Syto, R.; Schwartz, J.; Carr, D.; James, L.; Kirschmeier, P. *J. Biol. Chem.* **1995**, *270*, 30611, Ras proteins were visualized using AttoPhos (JBL Scientific, Inc., San Luis Obispo, CA) and quantified on a STORM phosphorimaging device (Molecular Devices, Sunnyvale, CA). IC_{50} values were calculated by fitting the data to the Michaelis–Menten equation using the non-linear regression analysis program Kaleidagraph (Synergy Software, Essex Junction, VT). All compounds were tested at least two times. The data are reported as the average of multiple determinations ±standard deviation (SD).
9. Protein Data Bank (PDB) file name of FTase X-ray structure is 105 M.
10. Taveras, A. G.; Kirchsmeier, P.; Baum, C. M. *Curr. Top. Med. Chem.* **2003**, *3*, 1103.
11. (a) Afonso, A.; Baldwin, J. J.; Doll, R. J.; Li, G.; Mallams, A. K.; Njoroge, F. G.; Rane, D. F.; Reader, J. C.; Rossman, R. R. WO9631478, **1996**; . *Chem. Abstr.* **1996**, *126*, 7997; (b) Cooper, A. B.; Doll, R. J.; Girijavallabhan, V. M.; Ganguly, A.; Reader, J. C.; Baldwin, J. J.; Huang, C.-Y. WO9857960, **1998**; . *Chem. Abstr.* **1998**, *130*, 81426.
12. To enhance the sensitivity of the FTase SPA assay, the following changes were made: Each reaction mixture (80 μl total) contained 50 mM Tris, pH 7.5, 5 mM $MgCl_2$, 5 μM $ZnCl_2$, 5 mM DTT, 0.01% (v/v) Triton X-100 (Sigma), and 176 nM [^{3}H]farnesyl pyrophosphate (NEN; 20 Ci/mmol). Purified FTase enzyme (280 pg, 30 pM final concentration) and inhibitor or DMSO control (5% v/v, final) were pre-incubated for 15 min at room temperature prior to the addition to the assay mix. The enzyme reaction was initiated with 20 μl of a solution containing 6.8 ng (100 nM final) biotin-CVLS followed by a 60 min incubation at 37 °C. Reactions were quenched with 150 μl of a cold suspension containing 250 mM EDTA (Digene), pH 8.0, 0.5% bovine serum albumin (Sigma), and 200 μg SPA beads.
13. Cell growth in soft agar was quantified as described in Du, W.; Lebowitz, P. F.; Prendergast, G. C. *Mol. Cell. Biol.* **1999**, *19*, 1831. Colonies were photographed using a video camera and tabulated using NIH Image software. IC_{50}s were calculated as described.[8]
14. To test for microsome stability, 5 μl of rat liver microsomes, with a cytochrome P450 content of 6.7 μM, was incubated for 60 min at 37 °C with 100 μl of 1 M KPi, pH 7.4, 100 μl freshly prepared 50 mM NADPH, and 10 μM compound (1 μl of a 10 mM solution in DMSO), all of which was adjusted to 1.0 ml in H_2O. The mixture was subsequently extracted with 200 μl dichloromethane and 150 μl of the organic phase was evaporated to dryness. The residue was dissolved in 25 μl methanol and analyzed by high performance liquid chromatography (HPLC) using a Phenomenex (Torrance, CA) ODS C-18 column. Samples were eluted for 27 min at a rate of 0.5 ml/min with a gradient of 44% B to 100% B where A consists of 0.1% TFA and B consists of 90% ACN containing 0.085% TFA. The percent of the compound remaining was quantified by comparison to samples extracted after 0 min incubation.
15. Oliyai, R.; Stella, V. J. *Ann. Rev. Pharmacol. Toxicol.* **1993**, *33*, 521.